International Journal of Cast Metals Research

ISSN: 1364-0461 (Print) 1743-1336 (Online) Journal homepage: https://www.tandfonline.com/loi/ycmr20

Investigation of casting/chill interfacial heat transfer during solidification of Al-11% Si alloy by inverse modelling and real-time x-ray imaging

K. Narayan Prabhu (Senior Lecturer) & John Campbell (Federal Mogul Professor of Casting Technology)

To cite this article: K. Narayan Prabhu (Senior Lecturer) & John Campbell (Federal Mogul Professor of Casting Technology) (1999) Investigation of casting/chill interfacial heat transfer during solidification of Al-11% Si alloy by inverse modelling and real-time x-ray imaging, International Journal of Cast Metals Research, 12:3, 137-143, DOI: 10.1080/13640461.1999.11819351

To link to this article: https://doi.org/10.1080/13640461.1999.11819351

Investigation of casting/chill interfacial heat transfer during solidification of Al-11% Si alloy by inverse modelling and real-time x-ray imaging

K. Narayan Prabhu†* and John Campbell‡
†*Senior Lecturer, Department of Metallurgical & Materials Engineering, Karnataka Regional Engineering College, Surathkal, Srinivasnagar 574 157, India Presently with the Manchester Materials Science Centre, University of Manchester and UMIST, United Kingdom as Research Associate*
‡*Federal Mogul Professor of Casting Technology, IRC in Materials for High Performance Applications, University of Birmingham, Edgbaston, Birmingham B15 2TT, United Kingdom*

Heat transfer at the casting/chill interface during solidification of Al-11% Si eutectic alloy (LM 6) was investigated. Experiments were carried out for various combinations of chill thickness, casting height and chill material. The thermal history at nodal locations in the chill was used to estimate the interfacial heat flux by inverse modelling. A new parameter called the heat flux penetration time was proposed to model the transformation of the interfacial condition from a perfect contact to a nonconforming contact. The heat transfer coefficient was modelled as a function of the chill thickness, casting height and the thermal diffusivity of the chill material.

Real time x-ray imaging technique was adopted to observe the casting/chill interface during solidification of the alloy. The video pictures indicate that a gas gap forms in the case of thin chills. The formation of the gap in thick chills could not be detected. The widths of the gap formed at the interface were measured by an image analyser which revealed that the width of the gap not only varies with time but also with position along the chill surface.

Keywords: casting/chill interface, interfacial heat flux, solidification, inverse modelling, gas gap, real-time x-ray imaging

Introduction

Modelling of heat transfer at the metal/mould interface is one of the critical problems in the simulation of casting solidification. When molten metal is poured into a mould, the rate at which it can lose heat is controlled by a number of resistances.[1] The resistances to heat flow from the interior of the casting can be grouped into five heads, namely, liquid metal, the solidified metal, the metal/mould interface, the mould and the surroundings of the mould. Resistances due to the liquid metal and surroundings of the mould can be negligible in practice. Furthermore, when the metal and the mould have good rates of conductance the boundary between the two becomes the region of dominant resistance. Thus in many casting processes, heat flow is controlled to a significant extent by the resistance at the metal/mould interface.[2–6] Gravity die casting, pressure die casting and continuous casting are some of the processes where product quality is affected by interfacial heat transfer conditions. Hence solidification modelling of these processes require a precise knowledge of the interface heat transfer characteristics.

During solidification of the casting there can exist three different thermal contact conditions at the casting/mould interface.

1 Conforming contact where the metal is in almost perfect contact, touching the mould surface at many locations
2 Nonconforming contact where the metal is in imperfect contact, touching the mould surface only at a few locations.
3 A clear gap where the skin of the solidifying casting physically separates from the mould wall surface.

The transformation of the interfacial condition from a nonconforming contact to a clear gas gap results in a drastic drop in the heat flow at the interface. At lower temperatures, the mode of heat transfer through the gas gap has been suggested to be predominantly due to conduction in the gap.[7]

Many researchers[8–10] have attempted to estimate the interfacial heat transfer coefficient. Inverse solution to the transient heat conduction equation and the measurement of mould and casting movements using suitable transducers to estimate the air gap thickness have been the most popular techniques. However so far no attempts have been made to observe the gas gap directly.

This paper is devoted to the modelling of heat flux transients at the casting/chill interface during solidification of Al-11% Si eutectic alloy (LM 6). LM 6 alloy is commonly used for large and intricate castings where corrosion resistance and ductility is required. It is convenient for this study because it freezes as a eutectic at the single temperature 577 °C. For the first time, a real-time x-ray imaging technique has been adopted to observe directly the formation of the gas gap and study its variation with time and position along the chill surface.

*Author for correspondence
e-mail: narayan_prabhu@hotmail.com

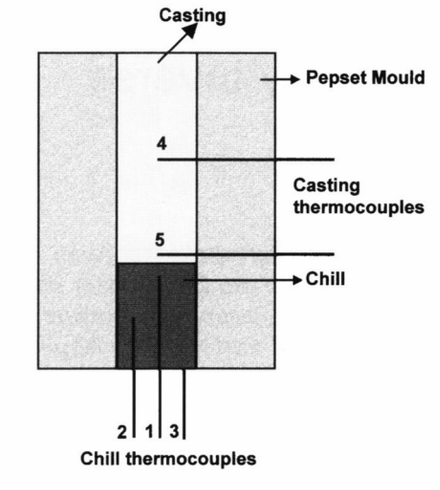

Fig. 1 Experimental set-up

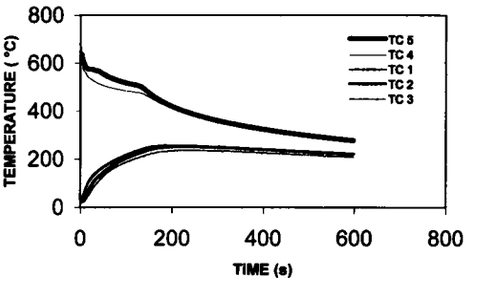

Fig. 2 Thermal history inside a casting and chill. Casting height: 50 mm, Chill: 80 mm copper

Experimental method

The alloy was melted in a clay/graphite crucible in a medium frequency induction furnace. The pouring temperature was maintained at 720 °C. The composition of the alloy is given below.

Si	Fe	Cu	Mn	Mg	Ni	Zn	Pb	Cr	Sn	Ti	Al
10.99	0.6	0.08	0.31	0.06	0.01	0.04	0.02	0.01	0.01	0.02	balance

Sand moulds were prepared using pepset process. Fig. 1 shows the mould with a cylindrical chill located at the base. One end of the chill was exposed to ambient conditions to simulate the conditions existing in the environment of a metallic mould. Mineral insulated chromel-alumel (K-Type) thermocouples of diameter 0.8 mm were located in the chill exactly at the finite difference nodal points. Table 1 gives the thermocouple locations in the chill material. Casting thermocouples 4 & 5 were located at the centre of the casting and 5 mm from the casting/chill interface respectively to monitor the solidification process. The tips of the thermocouples were protected by coating them with an alumina based paint. All of the thermocouples were interfaced to a computer-aided data acquisition system using compensating cables. For the direct observation of the formation of the air gap, a real-time 160 kV x-ray imaging system was used. The mould was placed between the x-ray source and a fluorescent screen, which converted the x-ray shadow image into a light image. The image thus obtained was electronically enhanced and recorded on videotape. The measurement of the width of the gas gap was carried out using an image analyser. Experiments were also carried out with the chill surface coated with a graphite based wash (Foseco Dycote 36) to study its influence on the gas gap.

The non-linear estimation technique of Beck[11] was adopted to analyse the transient heat transfer at the metal/mould interface. The one-dimensional Fourier heat conduction equation,

$$\frac{\partial}{\partial x}\left(\frac{\partial T}{\partial x}\right) = \rho C_p\left(\frac{\partial T}{\partial t}\right) \quad (1)$$

was solved inversely. In this inverse technique the surface heat flux density was estimated from a knowledge of measured temperatures inside a heat conducting solid. This was done by minimising, at regular finite difference time intervals, the function,

$$F(q) = \sum_{i=1}^{Mr}(T_n - Y_n)^2 \quad (2)$$

Table 1 Thermocouple locations from the casting/chill interface in the chill material

	Thermocouple Locations		
Thermocouple No	1	2	3
Radial Distance (mm)	0	−10	+10
Chill Thickness (mm)	Distance from the casting/chill interface in the chill material (mm)		
10	2	6	10
20	2	14	20
40	2	22	40
80	2	22	80

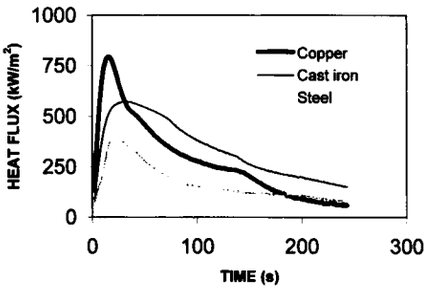

Fig. 3 Estimated heat flux transients for casting height $H_m = 50$ mm and chill height $H_c = 80$ mm

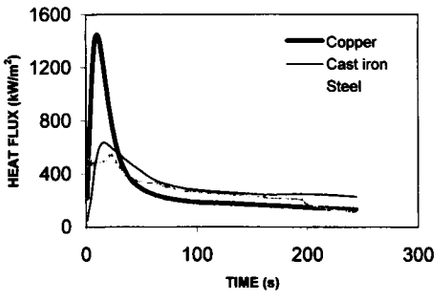

Fig. 5 Estimated heat flux transients for casting height $H_m = 200$ mm and chill height $H_c = 80$mm

where $M = \Delta\theta/\Delta t$ and $r =$ a small integer. T_n and Y_n are calculated and measured temperatures respectively at a location close to the surface of the solid. $\Delta\theta$ and Δt are the time steps for the estimation of heat flux and temperature respectively. Applying the condition for minimisation, the correction for heat flux (∇q) at each iteration step was estimated. The procedure was continued until the ratio ($\nabla q/q$) was less than a predetermined limit. The inverse modelling technique adopted here simultaneously yields the chill surface temperatures and the interfacial heat flux.

Results and discussion

Fig. 2 shows the typical thermal history inside a casting and chill during solidification of the alloy. Heat flux transients obtained with 80 mm and 10 mm copper, cast iron and steel chills are shown in figures 3–8. The heat flux transients show a peak soon after pouring. The results were checked for repeatability and Fig. 9 compares the heat flux curves generated for different runs of the same test conditions. It seems possible that the time of occurrence of the peak, denoted by t_g, is associated with the transformation of the interfacial condition from a conforming contact to a nonconforming contact or a gas gap. Assuming that the temperature of the casting skin in contact with the chill surface is at 577 °C (i.e. the freezing point of the alloy) at the time of occurrence of the peak heat flux, peak heat transfer coefficient is estimated from the equation,

$$h = \frac{q_{max}}{577 - T_c} \tag{3}$$

where h is the interfacial heat transfer coefficient corresponding to the peak heat flux q_{max} and T_c is the chill surface temperature.

Higher heat flux values were obtained with thinner chills, contrary to the expectations based on conventional wisdom. Copper and cast iron chills of 10 mm thickness appeared to show abnormally high values of heat flux transients and heat transfer coefficients. It seems that the 10 mm chill, being thin, is relatively flexible, so that as its front face heats up and expands, its face distorts towards the casting. As a result of this action, the improved contact with the casting will cause the front face to heat further, enhancing the distortion towards the casting. Thus this is a classic case of a runaway instability. The examination of the pattern of oxidation on the chill surface in contact with the casting revealed that the solidifying shell had contacted to the chill surface only at a few, limited points close to the centre of the chill. Conversely, the thick chills, having greater rigidity, appeared to keep their shape and location while the casting contracted away, leading to a nonconforming contact.

This strongly indicated that the heat flow was not truly one dimensional in the case of thin chills, so that the one-dimensional inverse heat conduction modelling was probably inappropriate, falsely indicating very high values of heat flux transients. This is also reflected in the thermal history of 10 mm chills where in most of the

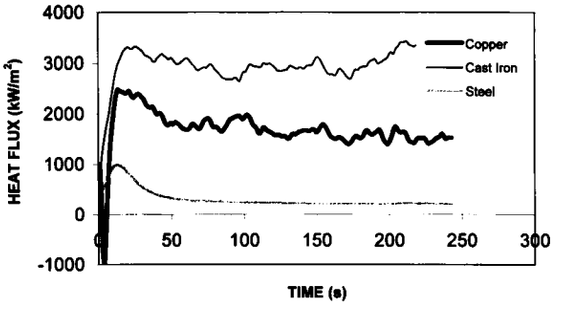

Fig. 4 Estimated heat flux transients for casting height $H_m = 50$ mm and chill height $H_c = 10$ mm

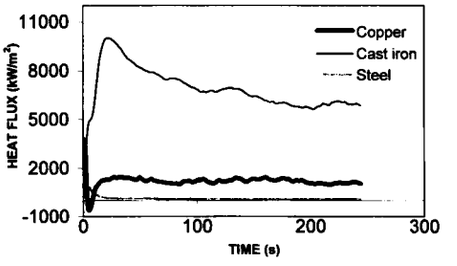

Fig. 6 Estimated heat flux transients for casting height $H_m = 200$ mm and chill height $H_c = 10$ mm

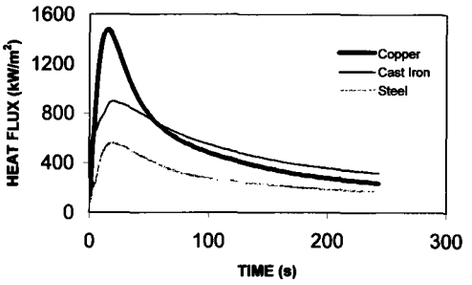

Fig. 7 Estimated heat flux transients for casting height $H_m = 500$ mm and chill height $H_c = 80$ mm

cases the thermocouple at the surrounding air/chill interface showed a higher temperature than the thermocouple located inside the chill material.

It was observed that only the chill height, H_c, and the thermal diffusivity, α, of the chill material had a significant effect on the time of formation of the gas gap t_g, irrespective of the metal height H_m. Fig. 10 shows the effect of $(H_c^2)/\alpha$ on t_g. It is interesting to note that the term $(H_c^2)/\alpha$ has the dimensions of time and effectively represents the heat penetration time in a given solid. The best-fit equation was found to be (excluding the data from 10 mm copper and cast iron chills):

$$t_g(s) = 1.5\left(\frac{H_c^2}{\alpha}\right)^{0.465} \tag{4}$$

or approximately,

$$t_g(s) = 1.5\left(\frac{H}{\alpha^{0.5}}\right) \tag{4a}$$

Furthermore, it can be seen that the metal height H_m, chill height H_c and the thermal diffusivity α of the chill strongly influenced the magnitude of the heat transfer coefficient. The variation of peak heat transfer coefficient with the term $(H_c/H_m)^2/\alpha$ is shown in Fig. 11. It seems likely that the dimensionless ratio of the chill height to metal height might be useful as a design parameter for solidification modelling. The best-fit regression equation (again excluding the results of 10 mm copper and cast iron chills) is;

$$h(W/m^2K) = 10\,801\left(\frac{(H_c/H_m)^2}{\alpha}\right)^{-0.187} \tag{5}$$

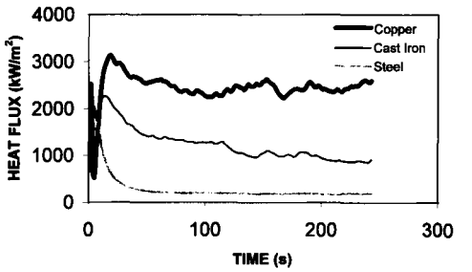

Fig. 8 Estimated heat flux transients for casting height $H_m = 500$ mm and chill height $H_c = 10$ mm

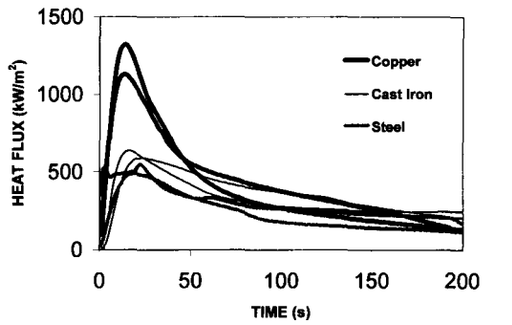

Fig. 9 Heat flux transients for different runs of the same test conditions. Casting height $H_m = 200$ mm and chilll height $= 80$ mm

Fig. 12 shows the variation of peak heat flux with the temperature drop (ΔT) at the casting/chill interface. The peak heat flux decreased linearly with increase in ΔT. The best-fit equation is;

$$q_{max}(kW/m^2) = -4.734(\Delta T) + 2901 \tag{6}$$

To observe the contact at the casting/chill interface directly, 200 mm high castings solidifying against 10 mm and 80 mm chills were subjected to real-time x-ray imaging technique. The video images captured for 10mm copper chills are shown in Figs 13–16.

The formation of the gap was detected only in the case of 10 mm chills. Assuming that the gap contained an equimolar mixture of air and hydrogen, the heat transfer coefficient was calculated using the relation,

$$h = k_g/\delta \tag{7}$$

where k_g is the thermal conductivity of the gas in the gap and δ is the gap width calculated by image analysis of the video frames of the real-time x-ray imaging experiments. The thermal conductivity of the gap at the casting/chill interface interface containing a equimolar mixture of air and hydrogen at 800 K was calculated using the thermal conductivity of hydrogen ($k_{hydrogen} = 0.378$ W/m K) and air ($k_{air} = 0.0573$ W/m K)[12] and was found to be 0.1548 W/m K. The data on the variation of gap width with time and position on the chill surface are given in Tables 2 & 3. The results clearly show that the

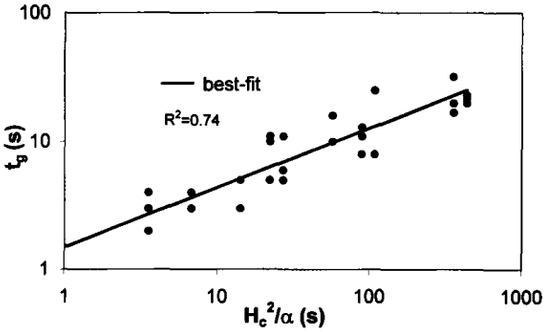

Fig. 10 Effect of $(H_c^2)/\alpha$ on t_g

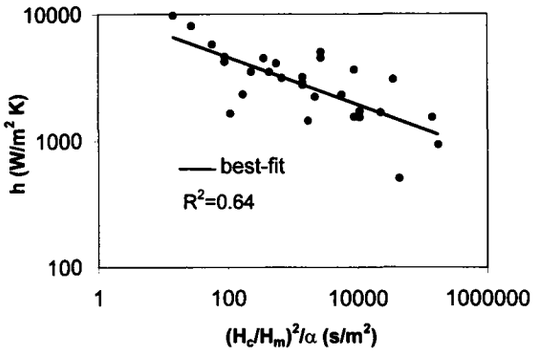

Fig. 11 Variation of heat transfer coefficient with $(H_c/H_m)^2/\alpha$

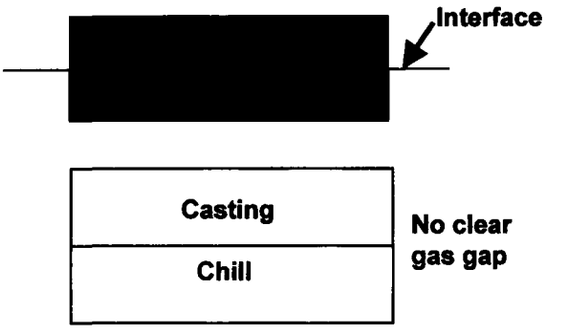

Fig. 13 Video image of the casting/chill interface. Chill: 80 mm copper, Time after pouring: 15 minutes

gas gap not only varies with time but also with position on the chill surface. This confirms, of course, that the heat transfer is not truly one dimensional in the case of thin chills. The heat transfer coefficient (h) was calculated using equation (7) at different time steps and locations shown in Tables 2 & 3. The values of h estimated in this manner are given in Tables 4 & 5. These values determined in this way are much less than those obtained by using the one-dimensional inverse analysis, and seem to be more realistic. The x-ray video also confirmed that normally, the liquid metal contacted the chill satisfactorily, only forming a gas gap later. However, in the case of graphite coated chills, there was initially a metal/chill coating reaction resulting in the expansion of a vapour bubble, of perhaps 1 ml volume, which temporarily displaced the melt from the chill surface (Fig. 14). After 6 seconds the vapour bubble deflated and the liquid appeared to resettle on the chill surface. This effect was ignored in the calculation of heat transfer coefficient.

Conclusion

1 Heat transfer analysis carried out during the solidification of Al-11% Si (LM 6) alloy showed the strong dependence of the heat flux transients on the height of the chill, the height of the casting and the thermal diffusivity of the chill material.

2 Heat flux transients showed a peak several seconds after pouring which could be attributed to the transformation of the interfacial conditions from a conforming contact to a nonconforming contact or a gas gap. The time of occurrence of peak heat flux was associated with the time of formation of gas gap (t_g). A new parameter called the heat penetration time given by $(H_c^2)/\alpha$ was proposed to assess t_g.

3 The magnitude of the heat transfer coefficient associated with the formation of gas gap was modelled as a function of the dimensionless ratio of the chill height to the metal height (H_c/H_m) and the thermal diffusivity (α) of the chill material.

4 Chills of only 10 mm thickness appeared to show very high heat flux transients compared to chills of 80 mm thickness. This was attributed to (i) the real effect of chill distortion and (ii) an apparent effect due to the heat flow being not truly one dimensional.

5 The observation of the casting/chill interface using real-time x-ray imaging technique indicated the formation of a clear gap in the case of 10 mm chills. Such a gap could not be detected in the case of 80 mm chills. The width of the gap varied not only with time but also with position along the chill surface, confirming the error in the assumption of one-dimensional heat transfer in the case of thin chills.

6 Heat transfer coefficients were estimated using the width of the gas gap and thermal conductivity of the gas in the gap. The estimated values seem to be more realistic than those obtained by inverse analysis.

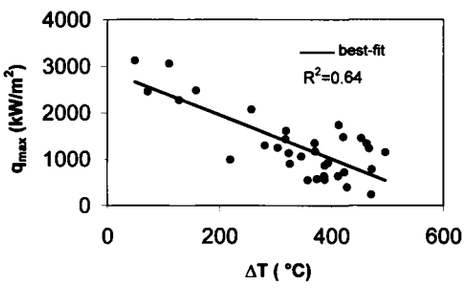

Fig. 12 Variation of peak heat flux with temperature drop at the casting/chill interface

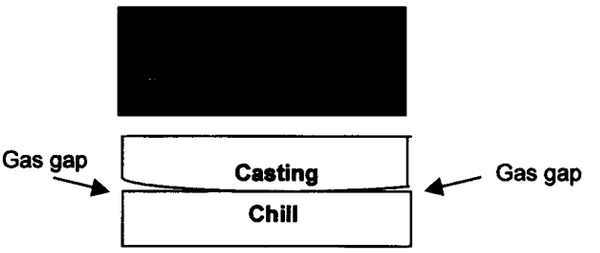

Fig. 14 Video image of the casting/chill interface. Chill: 10 mm copper uncoated, Time after pouring: 15 minutes

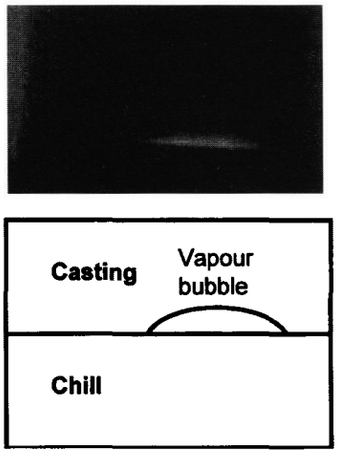

Fig. 15 Video image of the casting/chill interface. Chill: 10 mm copper with graphite coating , Time after pouring: 15 seconds

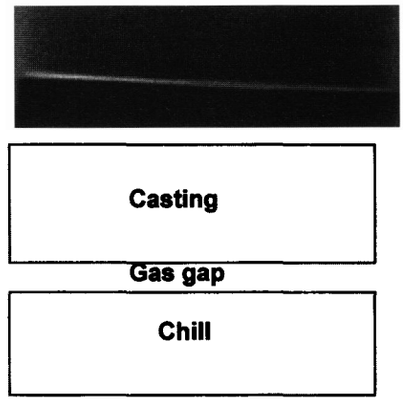

Fig. 16 Video image of the casting/chill interface. Chill : 10 mm copper with graphite coating , Time after pouring : 20 minutes

Table 2 Variation of gap width with time & position for 10 mm uncoated copper chill

Time (minutes)	Gas gap width δ (μm) at radius r (mm)			
	r = −25	r = −20	r = 0	r = 25
5	365	180	*	*
10	553	180	*	*
15	730	550	*	550

* Gap too small to measure (< 100 μm)

Table 3 Variation of gap width with time & position for 10 mm graphite coated copper chill

Time (minutes)	Gas gap width δ (μm) at radius r (mm)				
	r = −25	r = −20	r = −15	r = 0	r = 25
5	720	611	*	*	*
10	925	729	463	*	*
15	1036	922	922	922	768
20	1233	1233	1233	1233	768

* Gap too small to measure (< 100 μm)

Table 4 Heat transfer coeficients estimated from measurement of gas gap for 10 mm uncoated copper chill

Time (minutes)	Heat Transfer Coefficient h (W/m^2 K) at radius r (mm)			
	r = −25	r = −20	r = 0	r = 25
5	459	931	*	*
10	303	931	*	*
15	229	335	*	335

* Gap width too small to measure (< 100 μm)

Table 5 Heat transfer coeficients estimated from measurement of gas gap for 10 mm graphite coated copper chill

Time (minutes)	Heat Transfer Coefficient h (W/m^2 K) at radius r (mm)				
	r = −25	r = −20	r = −15	r = 0	r = 25
5	232	273	*	*	*
10	181	362	362	*	*
15	162	182	182	182	218
25	136	136	136	136	136

* Gap width too small to measure (< 100 μm)

Acknowledgements

The first author is grateful to the Department of Science and Technology, Government of India for awarding the BOYSCAST visiting research fellowship at the IRC in Materials, University of Birmingham. The authors thank Mr. Mike Flynn of the IRC for his excellent support and contributions in carrying out this investigation.

References

1. John Campbell, *Castings*, (Butterworth-Heinemann, Oxford,1991), pp. 125–128.
2. K. Ho and R.D. Pehlke, "Metal-Mold Interfacial Heat Transfer", *Metall. Trans. B*, 1985, **16B,** pp. 585–594.
3. T. S. Prasanna Kumar and K. Narayan Prabhu, "Heat Flux Transients at the Casting/Chill Interface during Solidification of Aluminium Base Alloys", *Metall. Trans. B*, 1991, **22B,** pp. 717–722.
4. J. Campbell, "Solidification Modelling: Current Limitations and Future Potential", *Mater. Sci. Technol.*, 1991, **7,** pp. 885–894.
5. S. W. Hao, Z. Q. Zhang, J. Y.Chen and P. C. Liu, "Heat Transfer at the Metal/Mold Interface in Ductile Iron", *AFS Transactions*, 1987, **95,** pp. 601–608.
6. K. Narayan Prabhu, G. Srinivas and N. Venkataraman, "Modelling Heat Transfer and Solidification Behaviour of Gravity Diecast Al-Cu-Si Alloy (LM 21) plates", *AFS Trans.*, 1993, **101,** pp. 653–659 .
7. Y. Nishida, W. Droste and S. Engler, "The Air-Gap Formation at the Casting-Mold Interface and the Heat Transfer Mechanism through the Gap", *Metall. Trans. B*, 1986, **17B,** pp. 833–844.
8. J. C. Hwang, H. T.Chuang, S. H.Jong and W. S. Hwang, " Measurement of Heat Transfer Coefficient at Metal/Mold Interface during Casting", *AFS Trans.*, 1994, **102,** pp. 877–883.
9. T. X. Hou and R. D. Pehlke, "Determination of Mold-Metal Interfacial Heat Transfer and Simulation of Solidification of an Aluminium-13% Silicon Casting", *AFS Trans.*, 1988, **96,** pp. 129–136.
10. K. Ho and R. D. Pehlke, " Transient Methods for Determination of Metal-Mold Interfacial Heat Transfer", *AFS Trans.*, 1983, **91,** pp. 689–698.
11. J. V. Beck, "Nonlinear estimation applied to the nonlinear inverse heat conduction problem", *J. Heat Transfer*, 1970, **13,** pp. 703–716.
12. D. R. Poirier and G. H. Geiger, *Transport Phenomena in Materials Processing*, (The Minerals, Metals & Materials Society, Pennsylvania, 1994), pp. 619–620.

(Received 14 January 1999; accepted 12 July 1999)